On-site performance assessment of an exhaust air heat pump: impact of refrigerant leakage and key performance indicators

Frédéric Ransy [a], Kevin Sartor[a], Vincent Lemort[a]

[a]*Thermodynamics laboratory, Aerospace and Mechanical Engineering Department, University of Liege, Allée de la Découverte 17, Belgium*

This paper examines the in-situ performance of an EAHP installed in a residential building in Belgium. The EAHP produces hot water to heat the building, and produces the DHW which is stored in a hot water tank. Due to limited ventilation airflow, the heat pump heating capacity is limited to 1450 W. During the experimental campaign, a refrigerant leakage was identified, and the impact on the performance was monitored. The first part of the paper focuses on the description of the exhaust air heat pump technology, and on previous work conducted on experimental on-site characterization of EAHPs. The second part describes the case study, with a detailed description of the building and the HVAC system, with a focus on the design and the control of the system. The monitoring system is also explained. The third section details the results. The behavior of the heating system for typical days is first introduced. It is shown that the exhaust air heat pump operates continuously in winter, and that the electric resistance is alternatively switched on and off to cover the peaks of the heating demand. The indoor thermal comfort is analyzed and shown to be satisfactory both in winter and summer. However, the hot water set-point temperature is not reached in summer, due to a refrigerant leakage. The performance is analyzed through two performance indicators: the average weekly COP and heating capacity. The impact of the refrigerant leakage on performance is clearly shown, with a reduction of 60 % and 50 % of the heating capacity and the COP, respectively. In the fourth section, the performance is extrapolated for a typical meteorological year. In the simulation, the heat pump covers 78 % of the energy demand of the building, and 22 % is covered by the electric resistance. About 43 % of the electricity consumption is related to the heat pump, 43 % to the resistance and 14 % to the auxiliaries. The seasonal COP is calculated to be 2.3.

Keywords: exhaust air heat pump, on-site performance, refrigerant leakage

Nomenclature

List of Acronyms

ASHP	**A**ir **S**ource **H**eat **P**ump
AFDD	**A**utomated **F**ault **D**etection and **D**iagnosis
COP	**C**oefficient **O**f **P**erformance
DHW	**D**omestic **H**ot **W**ater
EAHP	**E**xhaust **A**ir **H**eat **P**ump
EPBD	**E**nergy **P**erformance of **B**uildings **D**irective
EU	**E**uropean **U**nion
FDD	**F**ault **D**etection and **D**iagnosis
HVAC	**H**eating, **V**entilation, **A**ir-**C**onditioning
HP	**H**eat **P**ump
SPF	**S**easonal **P**erformance **F**actor
TXV	**T**hermostatic **E**xpansion **V**alve

List of Symbols

cp_w	water heat capacity
$\dot{M}$	mass flow
$\dot{Q}$	thermal power
Q	thermal energy
RH	relative humidity
t	time
T	temperature
$\dot{W}$	electrical power
W	electrical energy

List of Subscripts

aux	auxiliaries
avg	average
cd	condenser
cp	compressor
el	electric
ex	exhaust
res	resistance
su	supply
vent	ventilator
w	water

Introduction

Background

Since the Industrial Revolution, human activities have significantly increased the concentration of greenhouse gases in the atmosphere. These gases cause the global average Earth temperature to rise. Indeed, the current global average temperature is 0.85 K higher than it was in the late 19th century (IPCC 2023). An increase of 2 K could lead to non-controllable, long-term climate effects such as changes in precipitations, heat waves, rising sea level, a decline in agricultural yields and fisheries resources, and so on. Consequently, the international community has recognized the need to keep global warming below 2 K.

In this context, the EU defined different objectives to reduce the greenhouse gas emissions progressively up to 2050 to become the first climate-neutral continent (EU commission 2023). As stated on the official EU website: “In 2023, the EU adopted a set of Commission proposals to make the EU's climate, energy, transport and taxation policies fit for reducing net greenhouse gas emissions by at least 55% by 2030, compared to 1990 levels.” Two key targets were defined: the use of renewable energies to replace fossil fuels and an improvement in energy efficiency. For the use of renewable energies, the objective is ambitious: “The revised Renewable Energy Directive EU/2023/2413 raises the EU's binding renewable target for 2030 to a minimum of 42.5%, up from the previous 32% target, with the aspiration to reach 45%.” For the energy efficiency, the objective is the following: “This target sets the goal of reducing EU final energy consumption by 11.7% by 2030, compared to the projected energy use for 2030 (based on the 2020 reference scenario).”

To implement these targets, buildings have an important role to play. Indeed, in the EU, buildings account for the highest amount of energy consumed and the most CO_2 emitted,

about 40 % of the energy consumption and 36 % of the CO_2 emissions (EU commission 2020). For this reason, buildings offer a significant potential for energy saving. In 2020, the EU defined a long-term renovation strategy, the renovation wave initiative (EU commission 2020), to transform the existing building stock into nearly-zero energy buildings by 2050.

The exhaust air heat pump technology

The deep renovation of existing buildings implies two main aspects: the renovation of the building envelope to decrease the transmission heat losses and increase the airtightness, and the substitution of existing heating systems with new energy-efficient and carbon-free systems. Generally, in the case of residential buildings, the renovated buildings are also equipped with a mechanical ventilation system because natural ventilation is no longer sufficient to ensure a good indoor air quality.

The low-energy buildings are characterized by much lower transmission heat losses compared to conventional buildings. However, the ventilation heat losses are almost the same, because the building needs to be ventilated as well. Generally, for the Belgian climate, the maximum heating demand does not exceed 4 kW in low-energy buildings. Furthermore, the energy consumption associated with domestic hot water systems remains constant irrespective of the building type. Indeed, the occupancy profile is the primary factor influencing hot water consumption.

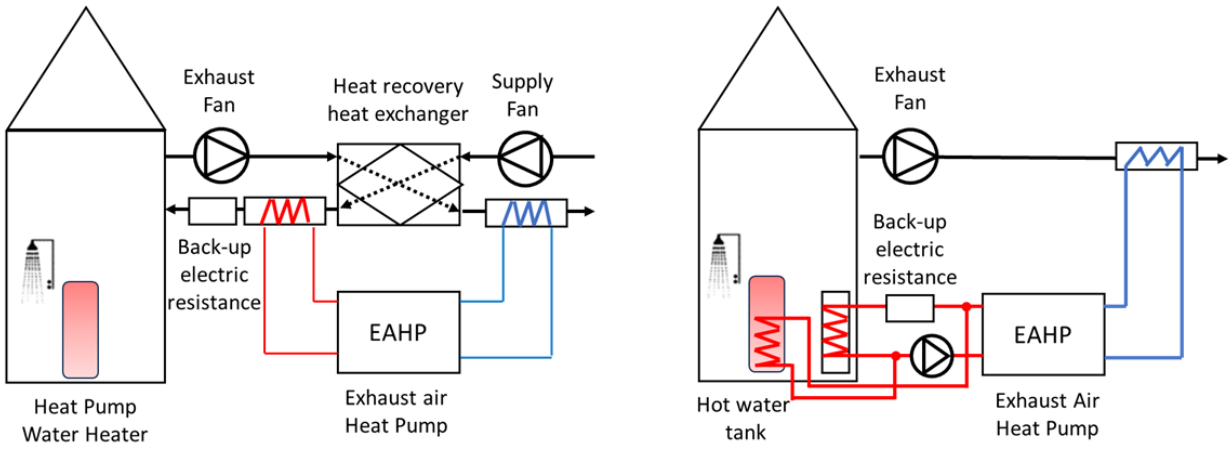

Figure 1: Concept of exhaust air heat pump. Left: air-to-air EAHP combined with a balanced ventilation system and a heat pump water heater Right: air-to-water EAHP combined with a simple exhaust ventilation system and a hot water tank

For these reasons, the heating and ventilation systems in highly efficient buildings may combine three aspects: a low heating capacity to prevent part-load operation, a heat recovery system integrated into the ventilation system and a high efficiency for the production of the domestic hot water. Within this framework, the EAHP technology is particularly suitable since it combines a ventilation with heat recovery and a heating system.

An exhaust air heat pump employs a closed-loop thermodynamic cycle to transfer heat from a cold medium, called the thermal source, to a hot medium, called the thermal sink. During the process, a mechanical work is consumed. In the case of an exhaust air heat pump, the cold medium is the exhaust air from the ventilation system. EAHPs are generally classified in two categories: air-to-air or air-to-water heat pumps. The two configurations are represented in Figure 1. In the first case (left in Figure 1), the heat pump provides hot and fresh air to heat directly the building. The heat pump is integrated with a balanced ventilation system with or without a heat recovery heat exchanger. In the second case (illustrated on the right of Figure 1), the heat pump is employed to produce hot water for sanitary use and/or to heat the building. The heat pump is combined with a simple exhaust ventilation system. In both systems, an additional backup electric

resistance is incorporated in the system because the EAHP heating capacity is not sufficient to cover the peak building heating demand during winter cold days.

Experimental on-site performance: previous work

Several authors studied the experimental on-site performance of EAHP while integrated in low energy buildings. In 2010, Fracastoro and Serraino (2010) presented the results of field monitoring of an air-to-air EAHP for Italy. A building model was developed to evaluate the annual performance of the EAHP, and 729 different case studies were considered. For all the case studies, the simulations indicated the necessity of a backup heating system. The authors demonstrated that the coverage factor (the energy provided by the EAHP divided by the total building energy demand) was the most important parameter influencing the seasonal efficiency. The correct design of the EAHP is therefore an important parameter to achieve good seasonal performance. In 2018, Dermentzis et al. (2018) presented the in-situ measurements of an air-to-air exhaust air heat pump combined with a balanced ventilation with heat recovery. The configuration is similar to the left part of Figure 1. The system comprised a 750 W heating capacity heat pump with a hermetic rotary compressor that could be operated in variable speed mode. A hot gas bypass was also implemented to defrost the evaporator if necessary. An additional electric post-heater was also placed in the supply air-duct to provide energy during peak periods. The DHW energy demands were covered by a central ASHP with a hot water loop. The whole system comprising the EAHP, the counterflow heat exchanger, the additional electric heater and the electric radiator in the bathroom had a SPF of 2.8. The in-situ measurements showed that 36 % of the energy consumption was related to the post-heater, indicating that the heat pump was not sufficient to provide the heating demand in winter. About 24 % of the energy consumption was dedicated to the fans, and 28 % was related to the compressor. Finally, about 6 % of the energy consumption was

related to the pre-heater (to avoid frost formation on the counterflow heat exchanger) and only 4 % for the heat pump defrosting cycles. In 2021, Shirani et al. (2021) presented the results of a field test monitoring of an air-to-air exhaust air heat pump. These data were used to validate a MATLAB/Simulink black-box model of the heat pump. This model was integrated in a building model to simulate the annual performance under different control strategies. The simulations showed that the moisture content of the air at the heat pump inlet has a significant impact on the EAHP performance. The control strategy of the electric backup resistance was also shown to be important to reach high efficiency. Concerning the control strategy of the heating system, the implementation of smart control strategies could reduce up to 40 % the electrical energy consumption of the system compared to conventional heating control methods.

The previous papers demonstrated the potential of air-to-air EAHPs in low-energy residential buildings. However, by definition, this category of EAHPs cannot produce the domestic hot water, which can represent a significant proportion of the total building energy demand. For this reason, the air-to-water EAHP technology offers a viable solution because it can recover the heat from the ventilation system while producing hot water for heating and DHW production. However, papers dealing with the on-site performance of air-to-water EAHP are limited in the literature. Pollet et al. (2015) monitored the field test performance of an air-to-water exhaust air heat pump (2.5 kW heating capacity at standard reference conditions). The heat pump was placed in a high-insulated apartments building. The heat pump produced the space heating and the domestic hot water. A backup gas boiler covered the peak demands in winter. The monitoring results were used to validate a building energy performance simulation tool. The backup boiler was shown to cover 33 % of the total energy demand, which is higher than the simulated value.

Impact of refrigerant leakage on heat pump performance: review

Refrigerant leakage in heat pump systems can have a significant impact on the heating capacity and the COP. This failure is part of common faults that can affect vapor compression systems. This topic, particularly the techniques utilized for the identification of such faults, has been intensively studied in the literature. In the late 1990s, Comstock and Braun (1999) provided a valuable experimental dataset concerning a 320 kW water chiller, incorporating both fault-free and faulty operation conditions, including refrigerant leakage. This dataset was utilized extensively to develop and validate FDD methods for chillers, and to identify performance degradation due to several faults. Comstock et al. (2001) analyzed the available data and demonstrated that refrigerant leakage has a negative impact on the efficiency of the chiller, and decreases the condensing pressure, the subcooling and the condenser approach temperature. This knowledge was then applied to air source heat pump systems. For instance, Llopis-Mengual and Navarro-Peris (2024) reported on the impact of single and multiple simultaneous faults in air source heat pumps. It was demonstrated that the deficit of refrigerant was responsible for lower evaporating and condensing pressures, lower subcooling and higher superheating values, lower mass flow rate and heating capacity, but an equivalent compressor consumption. Consequently, the COP is also decreased. The authors reported a decrease in the COP of between 8 and 15 % for a refrigerant leakage of 20 %. In another study, Mauro et al. (2023) modeled the refrigerant leak in a 2.6 kW residential air-air reversible heat pump incorporating detailed information regarding the impact on the refrigerant cycle. It is explained that, when facing a low refrigerant level, the thermostatic expansion valve is fed with vapor. This phenomenon results in valve choking and a decrease in the mass flow rate. Furthermore, the characteristic curve of the valve is modified, which changes

the equilibrium point between the compressor and the valve. This has been shown to decrease both the evaporating pressure and the mass flow rate, with a consequent negative impact on the COP and the heating capacity. Moreover, refrigerant leakage increases also the outlet temperature of the compressor. Considering a 30 % refrigerant leakage, the authors reported a 21 % and 12 % decrease in heating capacity and the COP, respectively. As demonstrated by Pelella and Mauro (2022) in another publication, a 26 % reduction in capacity was observed in the presence of a 40 % refrigerant leakage, accompanied by an augmentation of 12.5 K in evaporator outlet superheat.

In that context, the utilization of automated fault detection and diagnosis tools is valuable to minimize the maintenance costs by optimizing the planning of the interventions by technicians. Unfortunately, the development and the validation of an accurate AFDD tool is not straightforward. As explained by Yuill and Braun (2016), a substantial amount of data is required to train AFDD tools, accounting for various operating and fault conditions. The utilization of experimental data is a time-consuming and costly process. Moreover, the optimal distribution of input training data (type of faults, range of operating conditions) to allow the AFDD tool to perform well when deployed on-site is not clearly defined in the literature. A solution proposed by Yuill and Braun (2016) is to provide simulation-based input data for AFDD evaluation.

Objectives of the paper

The present paper investigates the in-situ performance of an air-to-water EAHP installed in a residential building in Belgium. The paper constitutes an extended version of a paper presented by the authors (Ransy et al. 2018). The first section describes the case study, by explaining the building geometry, the climate, the HVAC system, the design and the control of the heating system, and monitoring system. The second section shows the

results, with a particular focus on the behavior of the system during typical days, the thermal comfort and the system performance. During the tests, a refrigerant leakage occurred. This phenomenon is described and its impact on the performance is assessed. The third section discusses the results, including the calculation of the seasonal performance for a typical meteorological year.

The paper focuses on three aspects:

- The functional description of the EAHP to provide valuable information about the system control strategy, its advantages and limitations,
- The description of the refrigerant leakage and its impact on the performance,
- The estimation of the seasonal performance of the system and the relative contribution of each component in the system, i.e. the heat pump, the auxiliaries and the resistance.

For all these aspects, the available literature regarding air-water EAHPs is limited. This paper addresses these gaps. Fortunately, the information available in the literature regarding air-air EAHPs is a valuable source of information to criticize and validate the results obtained in this research.

Case study description

Building

The residential building case study was built in 2016. The detached house is composed of a wooden structure with two stories. As explained in the TABULA project (Cyx et al. 2011), the building geometry constitutes a conventional building design for new residential buildings. Table 1 provides the heated area for each room. The house includes also a third floor consisting of an unoccupied attic. In total, the heated area is 155 m² for a volume of 583 m³. The infiltration rate is not known, but a value n_{50} of 0.6 Vol/h can be assumed.

Table 1 : Heat area of each room in the building, adapted from Ransy et al. 2018

	Room	Heated Surface Area [m²]		Room	Heated Surface Area [m²]
Ground level	Living room	35	First stage	Bedroom 1	19
	Kitchen	13		Bedroom 2	16
	Study room	13		Storage room 1	12.5
	Laundry	8		Storage room 2	6
	Toilet	1.5		Bathroom	11
	Lobby	7		Night hall	13
	Total	77.5		Total	77.5

The building is energy-efficient. Indeed, the building overall heat transfer coefficient is 0.2 $W\ m^{-2}K^{-1}$ with a K-level of 17 (as specified in the Belgian EPBD, (Govaert et al. 2016)). Table 2 details the U-values and external area of the building envelope arranged by type of wall. The building is well insulated: 40 cm of spray-applied cellulose in the roof and the external walls, and 65 cm of foam glass in the concrete slab. The windows are made of triple glazing and aluminium frames that incorporate thermal breaks.

Table 2: U-values and external area of the building envelope, adapted from Ransy et al. 2018

Wall type	Composition	Area [m²]	U-value [W/m²-K]
Outer wall	Wood structure + 40 cm cellulose	158	0.11
Roof	Wood structure + 40 cm cellulose	127	0.15
Floor	Concrete slab floor + 65 cm cellular glass	82.7	0.1
Windows	Triple-glazed + aluminium frame	21	0.86

Climate

The Belgian climate is classified as maritime temperate, characterized by cold winters, mild summers, and a temperature difference of 15 K between the minimum and maximum monthly average temperatures. Common temperature levels for the design of HVAC systems is -10 °C dry temperature in heating mode and 30 °C/40 % dry temperature/relative humidity in cooling mode. The number of normalized annual heating and cooling degree days are 1835 and 140 in the 1990-2020 period, respectively. The monitoring period started the 1st of January 2019 and ended the 26th of December 2019.

This period was characterized by unusual high average temperature, unusual strong sunlight and normal precipitations. All the monthly average temperatures were higher in 2019 than for a typical year, except for the months of January, May and November. The winter 2019 was particularly mild, the temperature never fell below -6 °C. February was particularly warm with unusual high precipitations. This period was also characterized by a rare climatic phenomenon: three consecutive short heat waves in June, July and August.

Heating and ventilation system

The heating and ventilation system combines an exhaust ventilation system and an EAHP that produces hot water for DHW consumption and to heat the building. Figure 2 shows a representation of the system. In the following, the numerical values referenced in the text correspond to the values illustrated in Figure 2.

The exhaust ventilation system works by depressurizing the building utilizing an axial

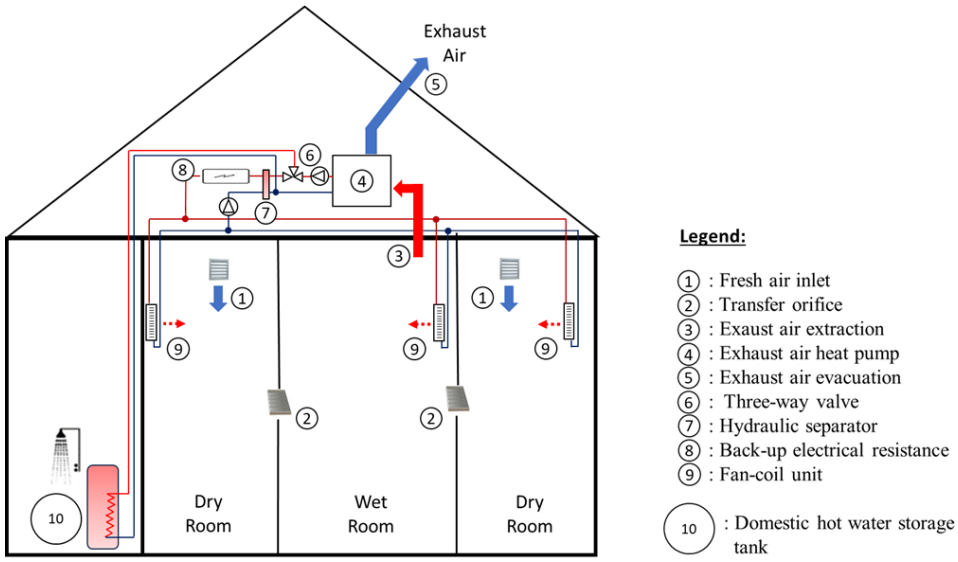

Figure 2: Representation of the heating and ventilation systems, adapted from Ransy et al. 2018

fan (3). In that way, the fresh air from the outside enters the dry areas in the building through the passive vents (1). The air is then transferred to the wet areas thanks to the transfer orifices (2). The polluted air is then collected by the exhaust ducting system in all the wet areas in the building (kitchen, bathroom, toilet), and sent to the inlet of the

EAHP (4). The air is cooled down, and evacuated (5). The heat pump includes classical components: a rolling piston compressor, a condenser (brazed plate heat exchanger), an evaporator (finned-tubed heat exchanger) and a TXV.

The hot water produced by the heat pump can be directed to either the DHW storage tank (10) or to the heating circuit (8 and 9). For this purpose, the hydraulic system in the house includes a hydraulic separator (7) to decouple the water mass flows from the primary and the secondary circuits, a three-way valve (6) that controls the heat pump operating mode, that can operate in 'space heating mode' or in 'domestic hot water production mode', a backup electric resistance (8) to provide additional heating in cold winter days, and fan-coil units (9) to heat the building. In the control strategy, the backup resistance can be activated, regardless the heat pump operating mode.

Design of the system

The design is divided into five phases. The ventilation ducting system is first designed. The Belgian Energy Performance of Buildings Directive (Govaert et al. 2016) imposes the nominal supply and extracted airflows in each room. In this particular case study, the nominal extracted airflow is 200 m^3/h. The repartition of the airflows between the zones is also imposed by the EPBD, and depends on the zone areas.

Secondly, once the nominal extracted airflow is known, the appropriate size of the heat pump is determined from the manufacturer catalogue. Indeed, the manufacturer proposes three heating capacities for three airflow rate values: 1250 W for 150 m^3/h, 1500 W for 200 m^3/h and 1900 W for 300 m^3/h. These particular values were obtained to maximize the COP while maintaining the evaporator under non-frost conditions in nominal conditions (A20W35).

The heat pump heating capacity is not enough to cover the maximum building energy demand. Therefore, the system design incorporates a backup electric resistance. At -10

°C outside and 20 °C inside, the maximum building energy demand given by the EPBD is 4100 W. Consequently, the backup electric resistance power is fixed at 3000 W.

Fourthly, it is necessary to correctly design the fan-coil units to ensure the indoor comfort of each room. Two fan-coil units with a heating power of 2350 W (A20W50) are installed in the living room and the bathroom, respectively. Three fan-coil units with a heating power of 1090 W (A20W50) are installed in the office and the two bedrooms, respectively.

In the final step, the volume of the water tank is chosen. It depends on the number of occupants in the building. At the present time, two people are living in the house. A volume of 150 liters would have been sufficient, but a volume of 200 liters was ultimately chosen.

Control strategy

In this section, the control strategy of the ventilation and the heating systems are presented.

The ventilation system is composed of a central exhaust fan to create the ventilation airflow, ducts for transporting the air, disk valves to control the airflows extracted in each wet area, filters to prevent dirt accumulation in the ducts and the heat pump, and passive vents through the building walls to introduce the fresh air to the dry areas. The ventilation control strategy is designed to maintain the humidity in the bathroom in an acceptable range. The fan operates continuously. A humidistat is installed in the bathroom to regulate the humidity level. In conditions where the relative humidity is below 45 %, the fan is operated at a medium speed, which results in a medium ventilation airflow. If the relative humidity level exceeds 55 %, the fan is operated at the maximum allowable speed, resulting in a high ventilation airflow. The medium (or nominal) ventilation airflow has been measured at 200 m^3/h during commissioning. The airflow value was

adjusted by the heat pump manufacturer during the installation of the system in the house. The high ventilation airflow value results from the equilibrium between the fan and the ducting system. It was measured at 300 m^3/h.

The control strategy of the heat pump and the backup resistance is more complex. The configuration of the three-way valve (6 in Figure 2) determines the heat pump operational mode, whether for space heating or domestic hot water production.

When the heat pump is activated to produce domestic hot water, the produced thermal energy is stored in the 200-liter water storage tank which has a set-point temperature of 50 °C. The DHW production mode is activated exclusively during the night, typically from 10 PM to 4:30 AM. During this period, the heat pump outlet temperature varies from 35 °C to 55 °C.

During the day, the heat pump is activated to heat the building. The control strategy maintains the outlet water temperature between 40 and 45 °C. The living room temperature is maintained around 20 °C with a hysteresis of 1 K. The set-point is monitored by a central thermostat, which activates the pump in the hydraulic network through an ON/OFF logic. A second sensor measures the heat pump inlet water temperature, which is maintained around the set-point of 39.5 °C through an ON/OFF activation logic of the heat pump with a hysteresis of 2 K.

In case of the heat pump capacity is lower than the building demand, the backup electric resistance is switched on. It is activated through an ON/OFF activation logic to maintain the resistance outlet temperature around the set-point of 43 °C with a hysteresis of 2 K. This control design ensures that the resistance is activated only if the heat pump is already switched on.

Fan-coil units regulate their fan speed to vary the heat emission and maintain the room set-point temperature of 20 °C.

Monitoring system

Several sensors are placed in the building and near the heat pump to assess its performance and the thermal comfort of the occupants. Figure 3 shows the sensor positioning.

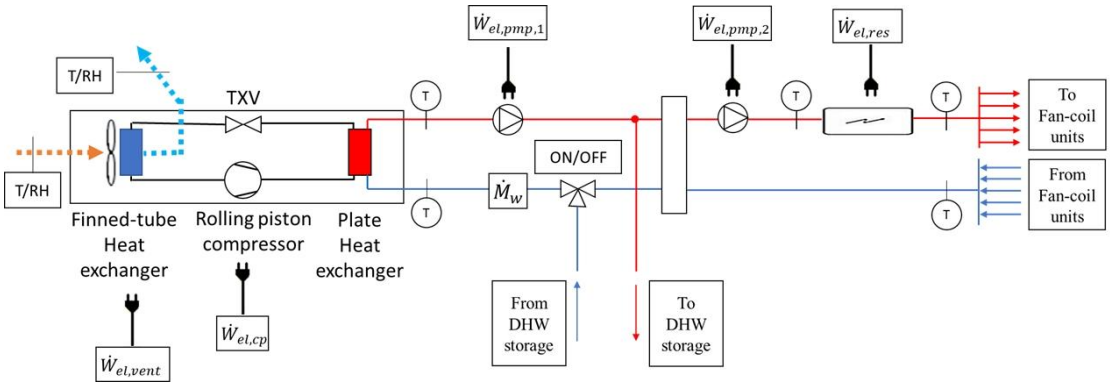

Figure 3: Position of the sensors used to measure the on-site performance of the heat pump, , adapted from Ransy et al. 2018

Digital temperature sensors are placed to measure the water temperature at the supply and the exhaust of the heat pump, at the supply and the exhaust of the backup resistance, and at the return of the heating system. The water temperature is not directly measured inside the pipes. Instead, the sensors are directly attached to the surface of the pipes and insulated from the environment. Thermal paste is added between the sensor and the surface of the pipe to minimize the thermal resistance. The pipe, made out of brass, minimizes the measurement error. A mass flow meter measures the water mass flow rate to calculate the heating capacity. The electrical consumption is measured by means of three digital electric meters placed on the compressor, the backup resistance and on the whole system. The temperature and humidity is also measured in four zones in the building: the living room, the bathroom, the office and the bedroom. Two digital temperature/humidity sensors measure the air inlet and outlet conditions of the heat pump. Table 3 shows the accuracies of the sensors. The acquisition system, consisting of a microcontroller, connects to the sensors each minute and store the values on cloud storage. As the

measurement system is of an experimental nature, it encountered numerous network connection disruptions. As the data was not locally stored, some data is missing during certain weeks.

Table 3: Accuracy of the sensors, adapted from Ransy et al. 2018

Measurement	Air humidity	Air temperature	Other temperature	Temperature difference	Water flow meter	Power consumption meter
Accuracy	2 %	0.3 K	1 K	0.5 K	2 %	1 %

Results

Behavior for typical days

Figure 4 illustrates the control logic of the heat pump and the backup resistance. The bottom part of the figure illustrates the time evolution of the thermal energy output of the

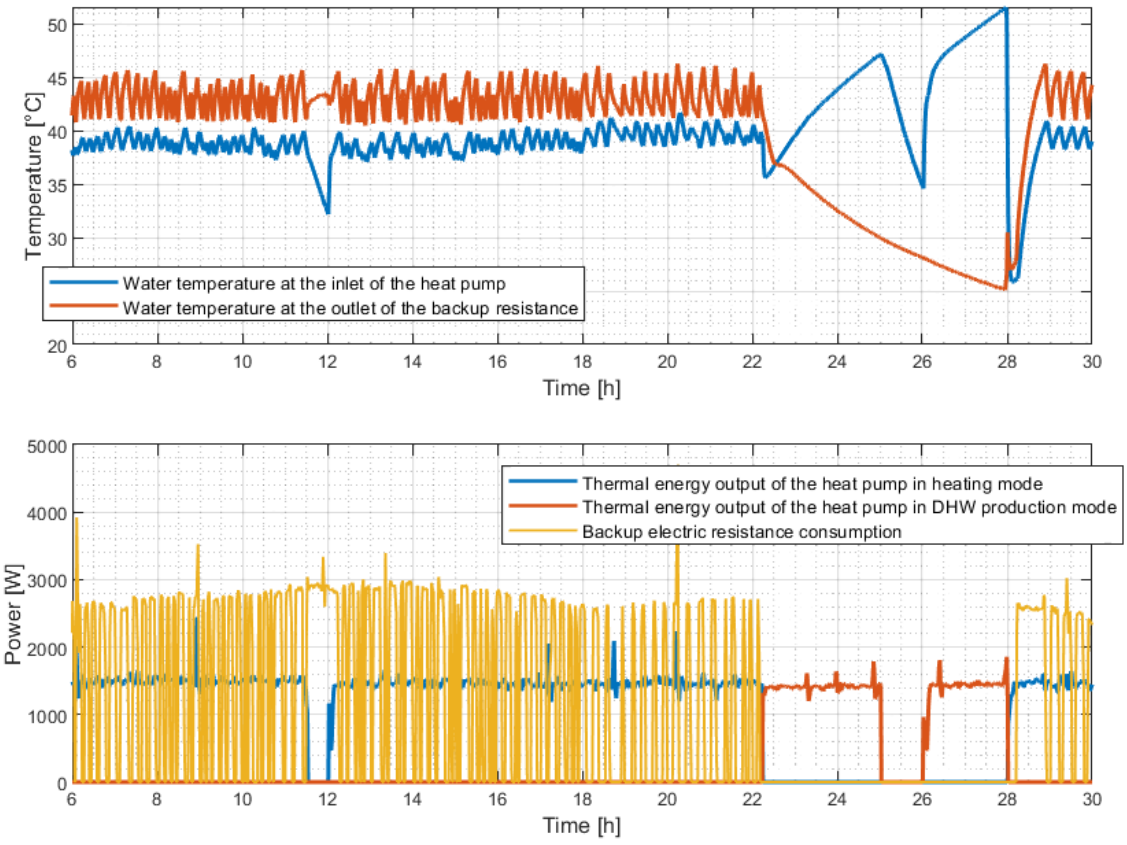

Figure 4: Example of thermal and electrical powers (bottom) and water temperature evolutions (top) during a cold outdoor temperature day (-3 °C in average)

heat pump, both in heating and DHW production modes, and the electrical consumption of the backup resistance.

The time period corresponds to a cold day (-3 °C in average outdoor). The measured heating capacity of the heat pump remains constant at 1500 W. For an unknown reason, the heat pump is switched off every day from 1 AM to 2 AM, and from 11:30 AM to 12:00 AM. The DWH production mode is activated only the night, from 10 PM to 4:30 AM. The rest of day, the heat pump is operated in heating mode. The backup resistance is activated only if the heat pump is in heating mode. The electrical consumption of this device fluctuates between 0 and 3000 W. The top part of the figure represents the time evolution of water temperatures at the inlet of the heat pump and the outlet of the resistance. During the day, the building heating demand being high during this cold day, the power provided by the heat pump is not sufficient. The backup resistance is then

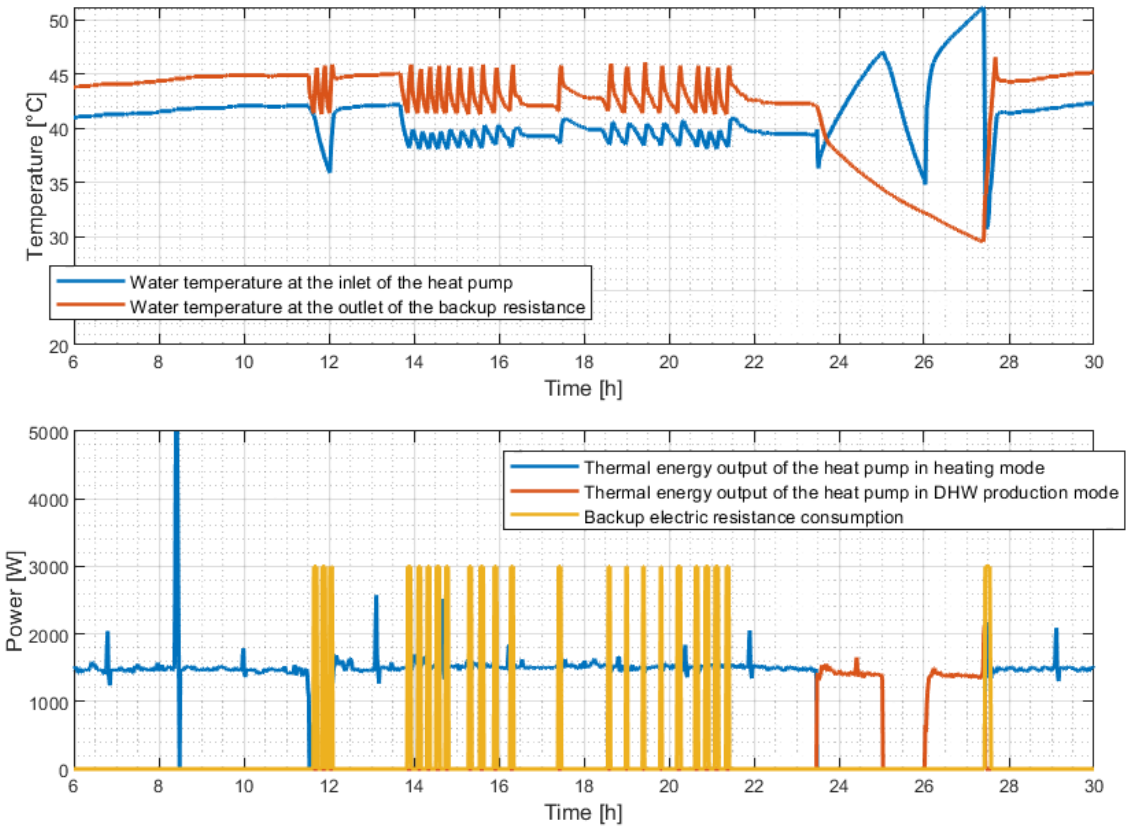

Figure 5: Example of thermal and electrical powers (bottom) and water temperature evolutions (top) during a mild outdoor temperature day (8 °C in average)

switched alternatively ON and OFF in order to maintain the temperature at the outlet between 41 and 45 °C. During the night, the heat pump is activated to produce the domestic hot water. Consequently, the heat pump outlet temperature increases slowly from 36 to 52 °C.

Figure 5 represents the same measurement data, but for another day characterized by a mild outdoor temperature (8 °C in average outdoor). The building energy demand is, in that case, lower. Again, the heat pump provides a constant heating capacity of 1500 W. In the morning, from 5 AM to 11 AM, the resistance is not switched on, and the temperature levels both at the heat pump inlet and the resistance outlet are smooth. At that moment, the building demand is equal to the heat pump delivered heating capacity. After 2 PM, the resistance is alternatively switched ON and OFF and the temperature levels are fluctuating a lot. The number of ON/OFF switches is significantly reduced during the mild outdoor temperature day in comparison to the cold temperature day.

Thermal comfort

The thermal comfort is evaluated through two key variables: the indoor air temperature and the delivery temperature of the domestic hot water. To that end, four temperature and humidity dataloggers are placed in the living room, the office, the occupied bedroom and the bathroom. The data is recorded at 30-minute intervals and downloaded through an USB interface every 6 months. The temperature of the delivered domestic hot water is also monitored at one-minute intervals.

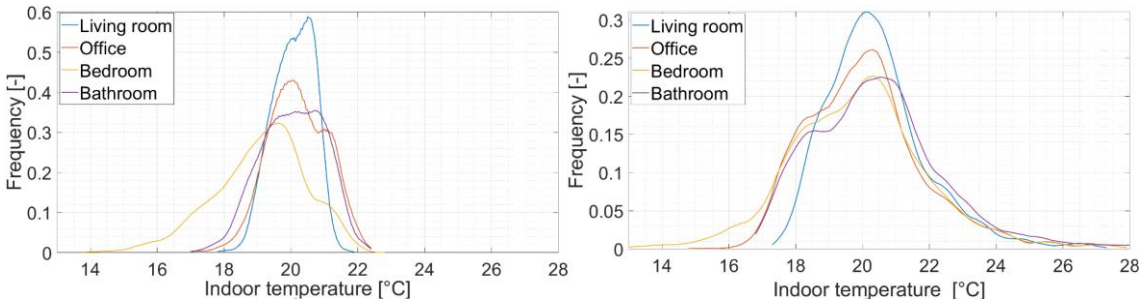

Figure 6: Frequency distribution of the indoor temperature measured by the four sensors. Left: winter. Right: summer

Figure 6 shows the frequency distribution of the indoor air temperature for the four sensors in winter and summer. The average temperature in the living room is 20 °C in winter and 20.4 °C in summer, with a standard deviation of 0.6 K and 1.5 K, respectively. The minimum and maximum temperatures are 17.2 °C and 27.3 °C, respectively. The temperature in the living room is controlled by a thermostat, with a set-point of 20 °C and a hysteresis of 1 K. The measurements show that the heating system is able to maintain the temperature around the set-point during the entire winter period. In summer, despite the three consecutive heat waves, the indoor temperature exceeded the limit of 25 °C only during 54 hours throughout the entire year. The risk of overheating is therefore limited. In summer, it is surprising to measure temperatures in the range 17-19 °C. It is because the control strategy allows a lower set-point temperature of 18 °C during the night. In April and September, the heating system was off, but the nights were cold, and the indoor temperature could drop below 18 °C. In winter, the frequency distributions of the temperatures in the bathroom and the office are similar. The living room, the office and the bathroom share the same average temperature, 20 °C. However, the standard deviations are slightly higher, 0.9 K for the office and 1 K in the bathroom. It means that the fluctuations around the set-point are higher in these two rooms. In winter, the shape of the frequency distribution of the bedroom is different from the three other distributions. The curve is shifted towards the left. The average temperature is 19.1 °C with a standard deviation of 1.4 K. Very cold temperatures between 12 et 14 °C are recorded. A substantial number of observed values are in the range 14-18 °C, which is low and not comfortable. These low values are explained by the choice of the occupants: the bedroom is not heated in winter. The analysis on the temperature recording shows a correct sizing of the heating system and the fan-coil units.

The house owners decided to fix the minimum hot water temperature at 52 °C. Figure 7 shows the maximum hot water temperature delivered by the heat pump on a weekly basis. From the week 1 until the week 27, the heat pump can provide hot water at the satisfactory temperature level of 52 °C. Then, from the week 35 to 39, the delivered temperature starts to decrease, from 50 to 45 °C. This temperature is clearly not acceptable. The heat pump owner contacted a technician during the week 40 to fix the problem. From the week 40 to 42, the heat pump owner activated the backup electric resistance and the temperature rises to the value of 58 °C. During the week 43, the technician founds a micro-leakage of refrigerant. He fixed the leakage and the refrigerant was completely recharged. The leakage explains why the heat pump could not provide a sufficiently high temperature. After repairs, the heat pump operates normally from week 43 to week 52, producing hot water at 52 °C.

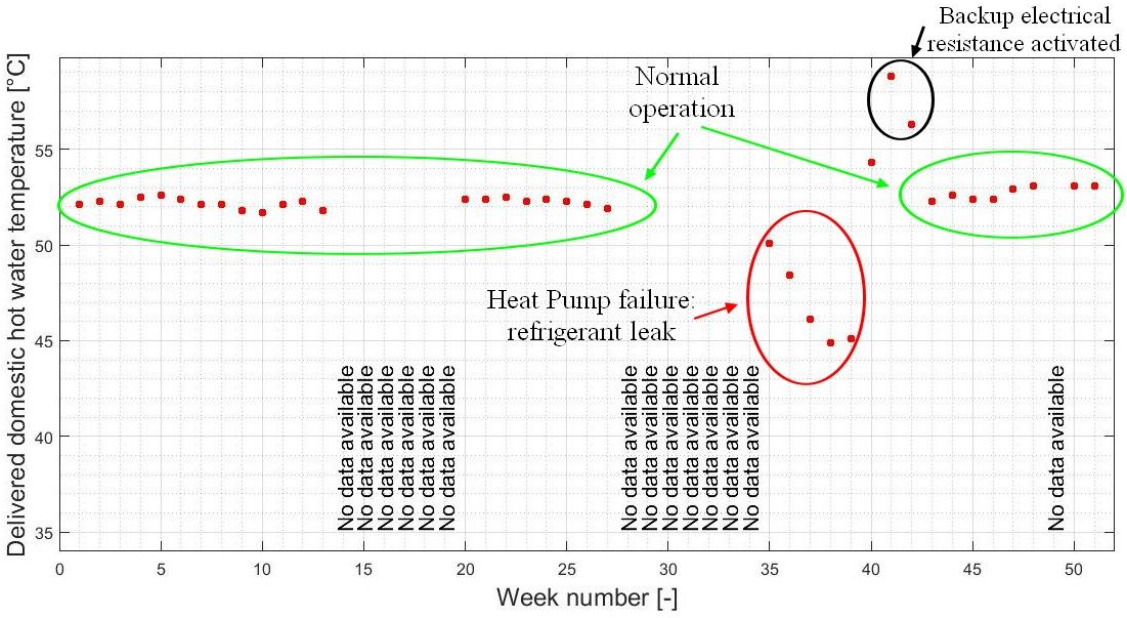

Figure 7: Delivered hot water temperature

Heat pump performance

The performance of the heat pump is defined by two criteria: the heating capacity and the COP. These performance indicators are averaged and presented over a weekly period.

The thermal energy output and the electrical energy consumed by the compressor over 1 week are firstly calculated as follows:

$$Q_{cd} = \int_{t_{start}}^{t_{end}} \dot{Q}_{cd}\ dt \tag{1}$$

$$E_{el,cp} = \int_{t_{start}}^{t_{end}} \dot{W}_{cp}\ dt \tag{2}$$

Where $\dot{Q}_{cd}$ is calculated with the measurements on the water side:

$$\dot{Q}_{cd} = \dot{M}_w\ cp_w \left(T_{w,ex,cd} - T_{w,su,cd}\right) \tag{3}$$

The interval $[t_{start}, t_{end}]$ represents the time interval between the Monday and the Sunday of each week. The average heating capacity and COP are defined as:

$$\dot{Q}_{cd,avg} = \frac{Q_{cd}}{t_{ON}} \tag{4}$$

$$COP_{avg} = \frac{Q_{cd}}{E_{el,cp}} \tag{5}$$

where t_{ON} is the heat pump run-time.

Figure 8 shows the weekly average COP, for the heating and the DHW production modes. The COP in heating mode is higher than the one in DHW production mode. The reason is a higher average output temperature in DHW production mode. From the week 1 to 13, the COP is relatively constant, comprised between 3.2 and 3.5 in DHW production, and between 3.5 and 4 in heating mode. After, from the week 20 to 27, the COP starts to decrease, reaching a value of 2.4 in week 27. Later in the year, from the week 35 to 40, the COP drops to the value of 1.5. It is due to the problem of refrigerant leakage. Following the repairs conducted in week 41, both the heating capacity and the COP returned to normal values.

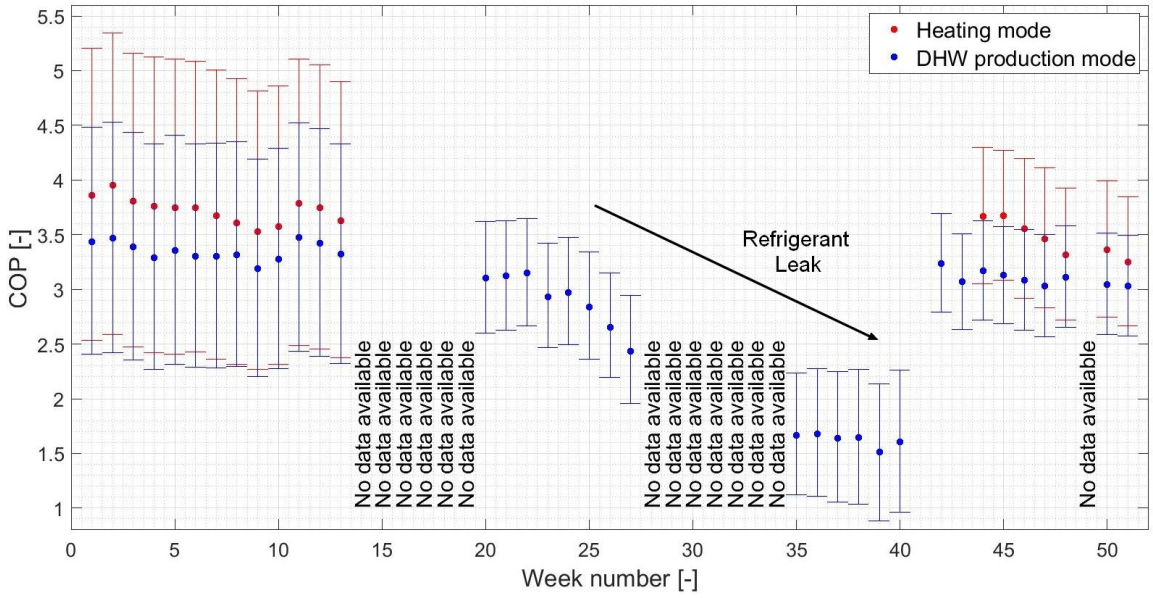

Figure 9: Weekly average COP of the heat pump

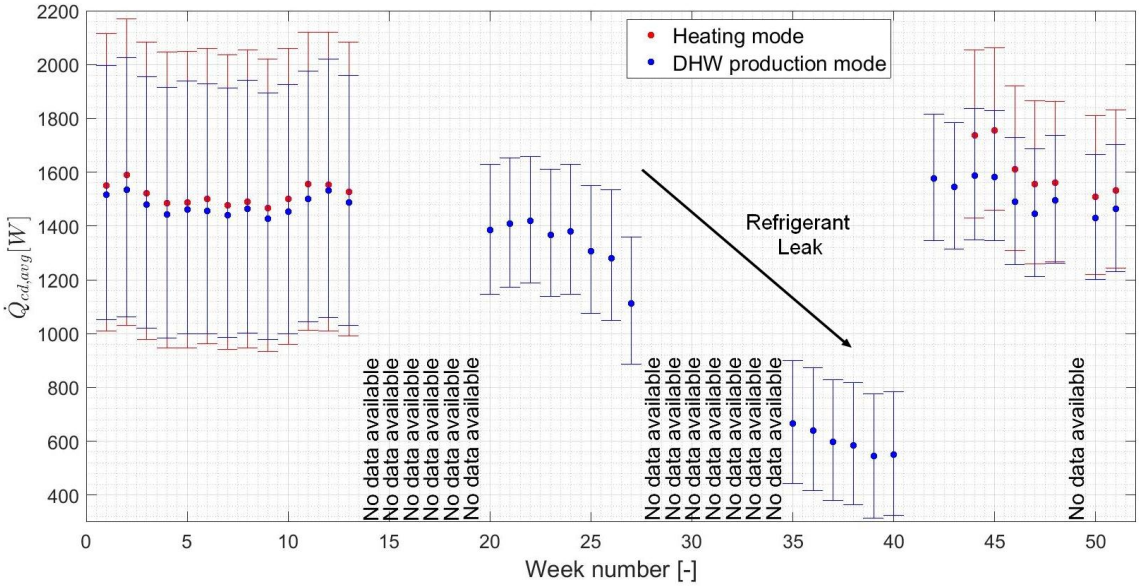

Figure 8: Weekly average heating capacity of the heat pump

Figure 9 shows the weekly average heating capacity, for the heating and the DHW production modes. The heating capacity in heating mode is slightly higher than the one in DHW production mode. The reason is a higher average output temperature in DHW production mode. The trends for the COP and the heating capacity are similar. From the week 1 to 13, the heating capacity remained relatively constant, ranging from 1400 to 1600 W. After, from the week 20 to 27, the heating capacity starts to decrease, reaching

the value of 1100 W the week 27. Later in the year, from the week 35 to 40, the situation is even worse. The heating capacity drops below the value of 550 W. This low heating capacity explains why the heat pump could not provide sufficiently hot water (see Figure 7). As explained in the previous section, this problem is due to a refrigerant leakage.

Whole system consumption

The whole system includes the heat pump, the backup resistance and the auxiliaries. Figure 10 represents the electrical energy consumption of all system components. In space heating mode, the consumption of the heat pump is almost constant, and varies between 50 and 70 kWh per week. The energy consumption of the electric resistance is much more variable over the weeks. In the winter season, from the week 1 to 7, the consumption varies from 60 to 140 kWh per week. In the mild season, the consumption is much lower, between 15 and 50 kWh per week.

The consumption of the resistance is strongly influenced by the outdoor temperature. Indeed, the energy consumption is inversely proportional to the outdoor temperature. The weekly consumption of the heat pump in domestic hot water production is almost constant, and varies between 10 and 15 kWh per week. The auxiliary equipment include the fan, the primary and secondary pumps. The electrical power consumptions of these components are relatively low, respectively 58, 6 and 45 W for the fan, the primary and the secondary pumps. However, the fan is operated continuously, and the two pumps are switched on during the entire winter period. Ultimately, the associated energy consumption cannot be neglected. In summer, the auxiliary equipment energy consumption is similar to the energy consumption of the EAHP for DHW production. Moreover, the auxiliary equipment consumes 150 % more energy in winter than in summer.

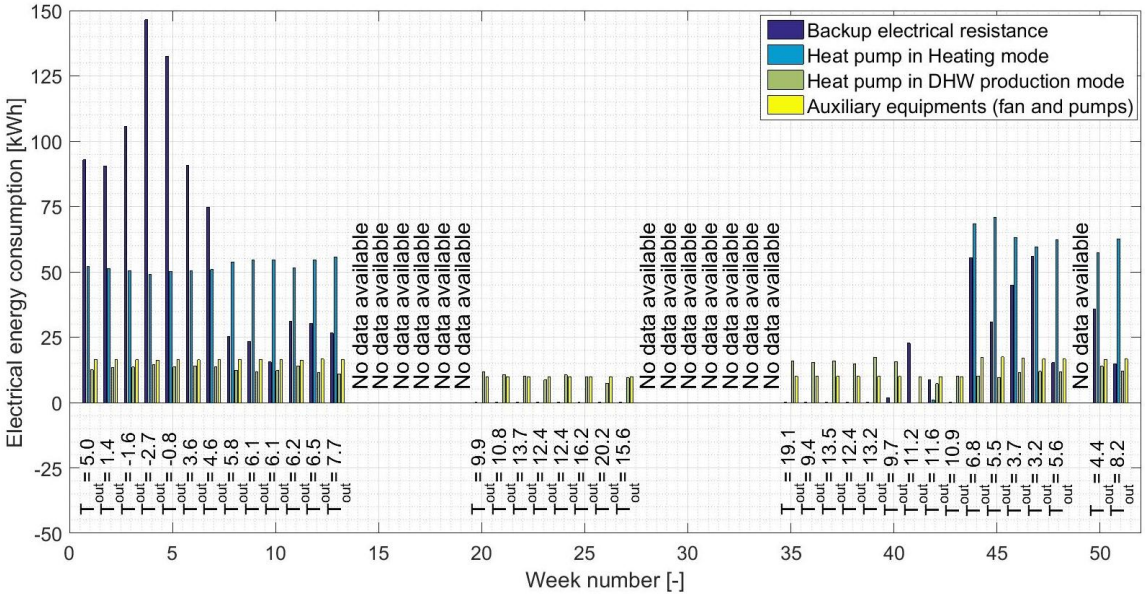

Figure 10: Weekly electrical energy consumption of all the systems: EAHP for heating and DHW production, backup resistance and auxiliaries

Discussion

The results showed that the indoor set-point temperature is reached during winter, meaning that the heating system, composed of the combination of the heat pump and the backup resistance, is correctly designed. However, as shown in Figure 4, the backup resistance is activated frequently in winter, while the heat pump operates continuously. Consequently, as shown in Figure 10, the monthly backup resistance consumption is high in winter, compared to the heat pump consumption. It can reduce the seasonal COP of the whole system.

Unfortunately, it is not possible to calculate the seasonal COP based on the measurements because of missing data and performance degradation due to refrigerant leakage. However, seasonal COP can be extrapolated for a typical meteorological year considering the following information directly measured on-site:

- In healthy conditions, the heating capacity is 1450 W (average value measured between weeks 1 and 13 and between weeks 42 to 51),
- The COP in healthy conditions is measured to be 3.6 in heating mode and 3.3 in domestic hot water production mode,
- The auxiliary consumption is measured at 58, 6 and 45 W for the fan, the primary and the secondary pumps, respectively, The fan operates continuously, and the pumps are activated when the heat pump is switched on,
- The building geometry and the construction materials are well documented.

The assumptions cited above should be treated with caution. In reality, the COP and heating capacity of the heat pump are subject to variation depending on the operating conditions. In order to take this into account, a detailed semi-empirical model of the heat pump is required, combined with a detailed model of the building. This methodology is beyond the scope of this paper, but represents an interesting potential for further developments. However, the assumptions can be criticized based on an analysis of the five inlet operating conditions. The frequency distributions for three of these variables are shown in Figure 11, for 1 complete year, from May 2019 to May 2020:

- The water flow rate depends on the equilibrium between the characteristic curve of the circulator and the resistance curve of the hydraulic network. As the frequency of the circulator is constant with no active element in the hydraulic network controlling the flow rate, the latter remains constant. Furthermore, the circuit being closed, the probability of heat exchanger clogging is limited, which guarantees a long-term constant flow rate.
- A similar analysis can be conducted for the airflow rate. The fan speed can take only two constant values: a nominal value, occurring most of the time, and a boost

value, which is activated only a few hours per day when the relative humidity in the bathroom is higher than 65 %. The level of fouling in the filters and the evaporator in the air circuit is limited, as the house occupants wash them every week to prevent a deterioration of the performance of their system. For practical reason related to limited available space, an air flow meter could not be installed. However, based on the above analysis, it can be assumed that the daily airflow rate remains constant on average during operation.

- The frequency distribution of the inlet water temperature throughout the heating period is a pseudo-Gaussian curve, with an mean value of 39.5 °C and a range between 38 °C and 44 °C (see the top of Figure 11). This indicates a constant operation at a temperature of 39.5°C with rapid variations (5 minutes) with a 2 K hysteresis due to ON/OFF operation of the backup resistance, as explained in the section entitled “behaviour for typical days”.
- Similar conclusions may be extrapolated for the other two variables. The frequency distributions for air temperature and humidity ratio at the inlet are Gaussian curves with average values of 20 °C and 7.5 g/kg, respectively. The indoor temperature is subject to variation, ranging from 17.5 °C to 24.5 °C. Temperatures around the average can be explained by the heating control system inducing a variation of 1 K around the setpoint of 20 °C. The night-time reduction at the beginning of the heating season explains the lower temperatures, and excess heat gains during the warm season explain the higher temperatures. Despite seasonal variations, the air inlet temperature is much less variable than for an outdoor air heat pump, where the air inlet temperature can vary from -10°C to 30 °C. The specific humidity shows the most significant relative variation. It varies from 5 to 14 g/kg, and the frequency distribution is right skewed.

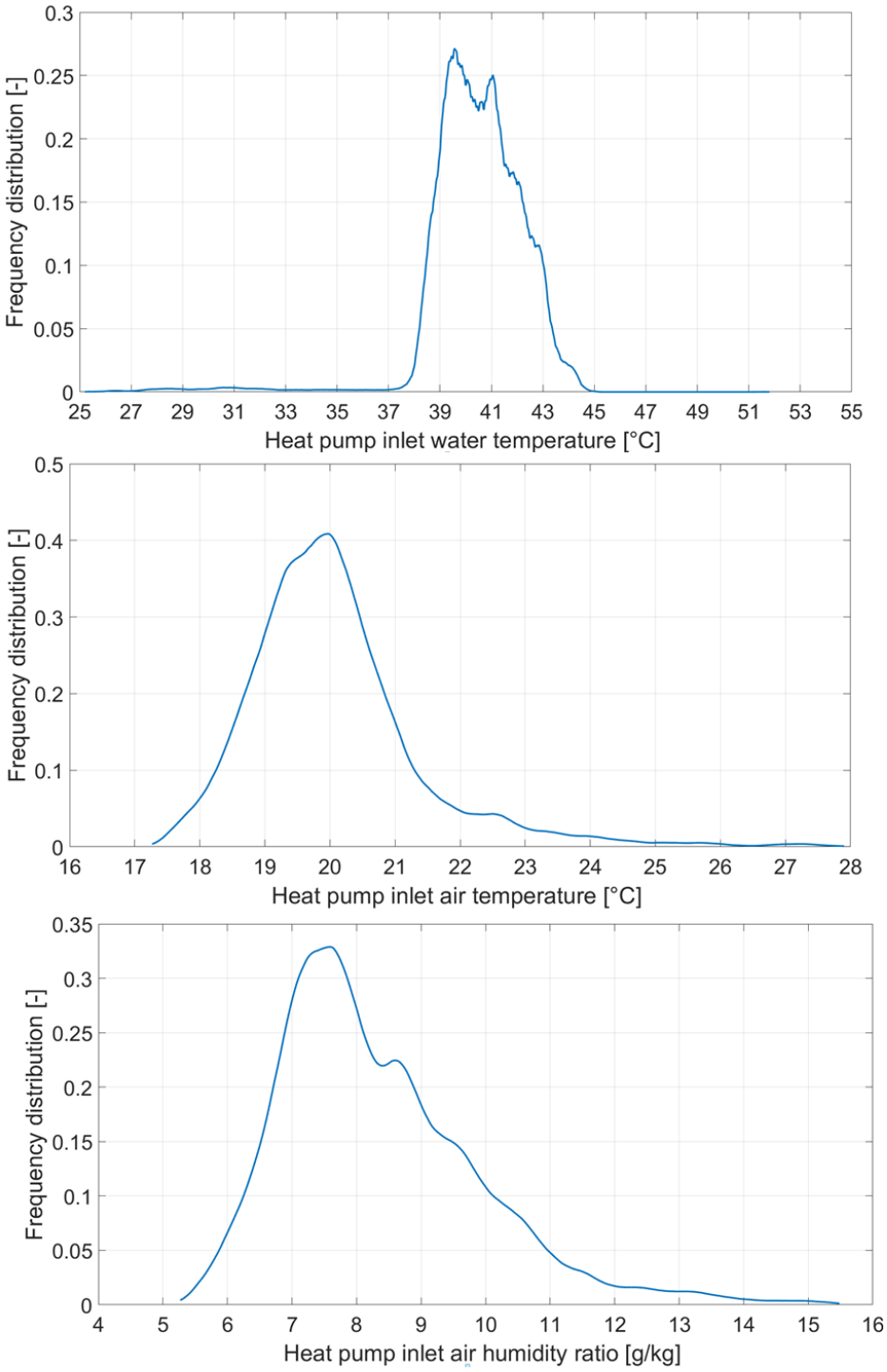

Figure 11: Frequency distribution of the heat pump inlet conditions (water temperature, air temperature and humidity ratio)

In order to calculate the seasonal COP, it is first necessary to calculate the building energy consumption. The latter is estimated based on the Energy Performance of Buildings (EPB) certificate (Govaert et al. 2016). This certificate, mandatory for new constructions

in Belgium, provides data on the energy consumption and the CO_2 emissions for buildings, considering normalized indoor climate conditions, weather conditions and occupancy profiles. The methodology considers the average monthly energy balance calculated on the entire building. The dynamic behaviour and the control logic are simplified. Table 4 shows the monthly building energy consumption for heating and domestic hot water in columns 2 and 3, respectively. Based on the heat pump heating capacity (1.45 kW) and supposing a maximum operation time of 24 hours/day, the maximum monthly thermal energy that can be provided by the heat pump is calculated. For example, for January, it is calculated as $Q_{HP,total} = 1.45 \,.\, 24 \,.\, 31 = 1079\ kWh$. If this amount of energy is not sufficient to cover the monthly building energy demand ($Q_{Heating} + Q_{DHW}$), the remaining part is covered by the electric resistance. The COP values in heating and DHW modes are then utilized to calculate the electrical consumption of the heat pump in both modes. The values are summarized in Table 4. The heat pump covers 78 % of the energy demand of the building, and 22 % is covered by the electric resistance. Concerning the electricity consumption, 43 % is related to the heat pump, 43 % to the resistance and 14 % to the auxiliaries. The seasonal system COP without auxiliaries is 2.3, and 1.94 considering the auxiliaries

A comparison can be drawn between these results and the in-situ measurement of Dermentzis et al. (2018). In their study, a SPF of 2.8 was obtained, to be compared with 1.96 in this study. Concerning the electrical energy consumption repartition, 28 % was dedicated to the compressor, 42 % to the backup resistance and 30 % to the auxiliaries. In this paper, the results are similar, but with a higher percentage relative to compressor (43 %) and a lower percentage for the auxiliaries (14 %). It is not surprising considering that, in the system of Dermentzis et al. (2018), an additional balanced ventilation system

is considered, which reduces the thermal energy demand of the building, but increases the fan consumption.

It seems that improvements could be implemented in the system tested in this paper. Indeed, the size of the compressor (the swept volume) could be increased. In that way, the refrigerant mass flow rate and the heating capacity increases, reducing the activations and the consumption of the backup resistance. Unfortunately, the airflow rate being fixed, the COP decreases, as the evaporating temperature decreases due to the higher refrigerant mass flow rate. Furthermore, the heat pump is more likely to encounter frost conditions, necessitating a dedicated defrost strategy and resulting in a decrease in the COP. Consequently, for each building type and occupancy, there exists an optimal compressor size that maximizes the SPF. This aspect represents the first perspective of this paper.

Table 4: Estimation of the monthly electrical consumption of the system

	$T_{out,avg}$ [°C]	$Q_{Heating}$ [kWh]	Q_{DHW} [kWh]	$Q_{HP,total}$ [kWh]	$Q_{HP,DHW}$ [kWh]	$Q_{HP,Heating}$ [kWh]	$W_{el,Res}$ [kWh]	$W_{el,HP,DHW}$ [kWh]	$W_{el,HP,Heating}$ [kWh]	$W_{el,aux}$ [kWh]
Jan	3.2	1545	180	1079	180	899	646	55	250	75
Feb	3.9	1278	162	974	162	812	466	49	226	68
Mar	5.9	1084	180	1079	180	899	185	55	250	75
Apr	9.2	548	174	722	174	548	0	53	152	61
May	13.3	74	180	254	180	74	0	55	21	46
Jun	16.2	0	174	174	174	0	0	53	0	42
Jul	17.6	0	180	180	180	0	0	55	0	43
Aug	17.6	0	180	180	180	0	0	55	0	43
Sep	15.2	10	174	184	174	10	0	53	3	42
Oct	11.2	376	180	556	180	376	0	55	104	57
Nov	6.3	1061	174	1044	174	870	191	53	242	73
Dec	3.5	1511	180	1079	180	899	612	55	250	75
Tot		7487	2118	7504	2118	5387	2100	642	1496	700
Avg	10.2									

The measurements showed also the impact on this technology of a refrigerant leakage. In the present experimental work, a 60 % reduction in heating capacity and a 50 % reduction in COP are observed. When compared to the literature (Llopis-Mengual and Navarro-Peris, Mauro et al., Pelella and Mauro), these values appear to be extremes, suggesting certainly an almost entirely uncharged system. Damage to the compressor may have been caused by motor overheating. The implementation of a predictive maintenance program

would have mitigated this risk. A second perspective of this paper is the development of this predictive maintenance tool specially designed for air-water EAHP. In the case of an EAHP producing domestic hot water stored in a water tank, the operating time of the heat pump in DHW production mode must be limited to the time needed to fully recharge the domestic hot water tank under normal operation. For example, considering a water tank with a volume of 150 litres at 50 °C and a cold water network temperature of 10 °C, the energy required to heat this water is 7 kWh. For a heat pump with a nominal heating capacity of 1.5 kW, the maximum operating time in domestic hot water production mode is 4 hours 40 minutes. More generally, a more detailed analysis of the energy content of the DHW tank using well-positioned sensors would allow further investigation. This concept could be studied more specifically and deployed on-site to be tested.

Conclusion

This paper proposes the analysis of the experimental on-site performance of an exhaust air heat pump producing hot water for space heating and domestic hot water production. The results showed a normal operation during the first weeks of the monitoring period with a heat pump heating capacity and COP of 1450 W and 3.6, respectively. However, a refrigerant leak was identified during the summer period, reducing the performance. Due to this problem and missing data, it was not possible to calculate the experimental seasonal system COP. However, an extrapolation for a typical meteorological year shows that the heat pump provides 78 % of the energy demand, and 22% is covered by the electric resistance. Auxiliaries account for 14% of the electrical consumption, 43% for the heat pump, and 43% for the electric resistance. Due to the significant consumption of the resistance, the seasonal COP of the entire system is 1.9, considering auxiliaries. This value is low in comparison to the literature, which means that the design of this system can be improved. Indeed, optimizing the compressor size would improve the annual

performance. The data presented in this paper could be utilised to validate models of the heat pump and the building, enabling different designs to be simulated and the best one selected. The paper highlighted the significant impact of refrigerant leakage on the heat pump performance, with reductions of 60 % in heating capacity and 50 % in COP being observed. This indicates that the system is almost empty. Such extreme values may lead to compressor damage due to motor overheating, a problem that could be mitigated through predictive maintenance. The development of a predictive maintenance tool specifically for air-to-water EAHP is proposed as a future research direction.

References

Comstock M.C, Braun J.E. 1999. Development of Analysis Tools for the Evaluation of Fault Detection and Diagnostics in Chillers ASHRAE Research Project RP-1043. Report# HL 99-20. Purdue University, Ray W. Herrick Laboratories, West Lafayette.

Comstock M.C, Braun J.E., Groll E.A. 2001. The sensitivity of chiller performance to common faults, International Journal of HVAC&R Research 7 (3), 263-279.

Cyx W., Renders N., Van Holm M., and Verbeke S. 2011. IEE TABULA - Typology Approach for Building Stock Energy Assessment. https://episcope.eu/ building-typology/country/be/.

Dermentzis G., Ochs F., Siegele D., and Feist W. 2018. Renovation with an innovative compact heating and ventilation system integrated into the façade - An in-situ monitoring case study. Energy and Buildings 165: 451-463

EU commission. 2020. A Renovation Wave for Europe - greening our buildings, creating jobs, improving lives. COMMUNICATION FROM THE COMMISSION TO THE EUROPEAN PARLIAMENT, THE COUNCIL, THE EUROPEAN ECONOMIC AND SOCIAL COMMITTEE AND THE COMMITTEE OF THE REGIONS.

EU commission. 2023. Energy roadmap 2050. https://energy.ec.europa.eu/.

Fracastoro G. V. and Serraino M. 2010. Energy analyses of buildings equipped with exhaust air heat pumps (EAHP). Energy and Buildings 42: 1283-1289.

Govaert M., Knipping G., Mortehan Y., Rolin I., and Rouard J-H. 2016. EPBD implementation in Belgium-Brussels Capital Region.

IPCC. 2023. Climate Change 2023: Synthesis Report. Contribution of Working Groups I, II and III to the Sixth Assessment Report of the Intergovernmental Panel on Climate Change.

Llopis-Mengual B., Navarro-Peris E. 2024. Selection of relevant features to detect and diagnose single and multiple simultaneous soft faults in air-source heat pumps. Applied Thermal Engineering, Volume 238, 121922.

Mauro A.W, Pelella F., Viscito L. 2023. Performance degradation of air source heat pumps under faulty conditions, Case Studies in Thermal Engineering, Volume 45, 103010.

Pelella F., Viscito L., and Mauro A. W. 2022. Combined effects of refrigerant leakages and fouling on air-source heat pump performances in cooling mode. Applied Thermal Engineering 204: 117965.

Pollet I., Coulier C., Vens A., and Grillet F. 2015. Residential demand controlled extract ventilation combined with heat recovery via a heat pump. *Proceedings of the 36th AIVC conference*. Madrid, Spain, pp. 830-840.

Ransy F, Sartor K., Gendebien S and Lemort V. 2018. Experimental On-site Performance and Numerical Analysis of a Mini Exhaust Air Heat Pump Integrated into a Low Energy Detached House. *International High Performance Buildings Conference, West Lafayette, IN, United States.* Paper #313.

Shirani A., Merzkirch A., Roesler J., Leyer S., Scholzen F., and Maas S. 2021. Experimental and analytical evaluation of exhaust air heat pumps in ventilation-based heating systems. Journal of Building Engineering 44: 102638.

Yuill D. P., Braun J. E. 2016. Effect of the distribution of faults and operating conditions on AFDD performance evaluations, Applied Thermal Engineering, Volume 106, Pages 1329-1336,